Research in Pharmaceutical Sciences, December 2024; 19(6): 754-765
Received: 08-09-2023
Peer Reviewed: 05-11-2023
Revised: 23-11-2023
Accepted: 23-11-2024
Published: 15-12-2024

School of Pharmacy & Pharmaceutical Sciences
Isfahan University of Medical Sciences

Original Article

Multiple ligands simultaneous molecular docking and dynamics approach to study the synergetic inhibitory of curcumin analogs on ErbB4 tyrosine phosphorylation

La Ode Aman[1,*], Netty Ino Ischak[2], Teti Sutriyati Tuloli[1], Arfan Arfan[3], and Aiyi Asnawi[4]

[1]*Department of Pharmacy, Faculty of Sport and Health, Universitas Negeri Gorontalo, Gorontalo, Indonesia.*
[2]*Department of Chemistry, Faculty of Matematics and Natural Sciences, Universitas Negeri Gorontalo, Gorontalo, Indonesia.*
[3]*Faculty of Pharmacy, Universitas Halu Oleo, Kendari, Indonesia.*
[4]*Faculty of Pharmacy, Universitas Bhakti Kencana, Bandung, Indonesia.*

Abstract

Background and purpose: Lapatinib (FMM) and 5-fluorouracil (5-FU) are anticancer drugs employed in a combination approach. FMM inhibits tyrosine phosphorylation of ErbB4 while 5-FU inhibits cell proliferation. This research aimed to investigate the potential of two compounds, namely (1E,4E)-1,5-bis (4-hydroxyphenyl) penta-1,4-dien-3-one (AC01) and (1E,4E)-1,5-bis (3,4-dihydroxy phenyl) penta-1,4-dien-3-one (AC02), both as individual inhibitors and combination partners with FMM, targeting ErbB4 inhibition. AC01 and AC02 were combined with FMM, which targets ErbB4. The combination of 5-FU with FMM served as a reference in this study.
Experimental approach: The research utilized computational simulation methods such as single and multiple ligands simultaneously docking and dynamics. Data analysis was performed using AutoDockTools and gmx_MMPBSA.
Findings/Results: Single docking results indicated that 5-FU exhibited the lowest binding affinity, while FMM demonstrated the highest. Simultaneous docking of AC01 and AC02 paired with FMM revealed their binding positions overlapping with the FMM-5-FU workspace. The FMM-AC01 and FMM-AC02 complexes exhibited slightly weaker binding affinities compared to FMM-5-FU. In combination with FMM, AC01 and AC02 occupied the ErbB4 activation loop, whereas 5-FU was outside the activation loop. Furthermore, in their interaction with ErbB4, AC02 exhibited slightly stronger binding than AC01, as confirmed by the average binding free energy calculations from molecular dynamics simulations.
Conclusion and implications: In conclusion, computational simulations indicated that both AC01 and AC02 have the potential to act as anticancer candidates, demonstrating ErbB4 inhibitory potential both as individual agents and in synergy with FMM.

Keywords: ErbB4; Simultaneously molecular docking; Simultaneously molecular dynamics.

INTRODUCTION

Cancer remains a paramount global health concern, with staggering numbers of new cases reported each year. In 2020 alone, there were 18.1 million new cancer cases worldwide, highlighting the urgent need for effective solutions (1). Among the most prevalent cancer types, breast cancer in women as well as lung, colorectal, and prostate cancer are at the forefront. Of these, breast cancer is well outstanding, with approximately 2.3 million women diagnosed in 2020, and it has accounted for nearly a quarter of all cancer cases and 15.5% of cancer-related deaths in women, making it the leading cause of both incidence and mortality (2-4).

*Corresponding author: L.O. Aman
Tel: +62-81321781245, Fax: +62-435821125
Email: laode_aman@ung.ac.id

Access this article online	
	Website: http://rps.mui.ac.ir
	DOI: 10.4103/RPS.RPS_191_23

ErbB4, also known as human epidermal growth factor receptor 4 (HER4), is a crucial player within the epidermal growth factor receptor (EGFR) family, particularly in breast cancer. The activation of ErbB4 significantly impacts the development, proliferation, and differentiation of breast cancer cells. This receptor is a part of the EGFR family, which also encompasses EGFR (ErbB1/HER1), ErbB2 (HER2/Neu), and ErbB3 (HER3) in humans (5). The normal function of ErbB receptors is integral to animal development, and the aberrant expression and activation of the receptors have been linked to various human cancers. Notably, the loss of ErbB4 function in mice results in defects in the heart, nervous system, and mammary glands (5-6). The ErbB family exerts its biological effects through the ligand-dependent activation of tyrosine kinase activity. ErbB receptors consist of an extracellular ligand-binding region, a transmembrane segment, a cytoplasmic kinase domain, and a tail with phosphorylated tyrosine residues upon activation, facilitating interactions with downstream effectors. Ligand binding in the extracellular region triggers the formation of ErbB homodimers and specific heterodimers, leading to cytoplasmic kinase activation and initiating intracellular signaling cascades (7,8).

In treating ErbB4-dependent breast tumors, targeting ERBB2 expression or tyrosine kinase activity has proven effective, even in cases resistant to other therapies. A range of ErbB4 kinase inhibitors exists such as lapatinib (FMM), afatinib, neratinib, and ibrutinib. FMM as one of the ErbB4 kinase inhibitors prevents ErbB4 kinase similarly to its interaction with EGFR, impeding ErbB4 phosphorylation and downstream signaling pathways. By inhibiting ErbB4 signaling, FMM has shown the ability to induce apoptosis in FMM-resistant breast cancer cells, highlighting its therapeutic potential (9). However, the intricate interplay among the ErbB family members and their overlapping functions poses challenges. Ligands that interact with ErbB4 may also bind to EGFR or ErbB3, and ErbB4 ligand binding can result in either ErbB4 homodimerization or heterodimerization with other ErbB family members (10). Consequently, finding novel compounds targeting specifically ErbB4 remains a formidable challenge in developing new anticancer drugs.

Accordingly, this study delved into the potential of two curcumin analogs, (1E,4E)-1,5-bis (4-hydroxyphenyl) penta-1,4-dien-3-one (AC01) and (1E,4E)-1,5-bis (3,4-dihydroxy phenyl) penta-1,4-dien-3-one (AC02), as promising candidates for ErbB4 inhibition in cancer therapy. We employed a computational approach known as multiple ligand simultaneous docking (MLSD) to investigate the effectiveness of curcumin analogs. This technique allows the study of the concurrent interaction of several ligands with a binding site of the macromolecule, mirroring the complex biochemical processes involved in combination dosing, a common practice in cancer therapy (11,12). By comparing binding orientations and assessing binding energies, MLSD provided valuable insights into the influence of inhibitors on ligand binding to the ErbB4 protein. The stability of the docking interactions was further scrutinized through multiple ligand molecular dynamics to clarify the potential of these compounds and revolutionize anticancer drug development.

MATERIALS AND METHODS

Data preparation

The data collection process for this study included retrieving the molecular structures of FMM, AC01, AC02, and 5-fluorouracil (5-FU) (Fig. 1) from the National Library of Medicine (https://pubchem.ncbi.nlm.nih.gov). The molecular structures of the ligands were obtained in 2D format, necessitating geometric optimization performed using Open Babel 3.1.1. Energy minimization was conducted using the chemical force field, with 1000 geometry optimization steps (13). The 3D structures of the ErbB4 protein were generated using the homology modelling technique, employing the Swiss-Model tool, accessible at https://swissmodel.expasy.org (14). The homology modelling template utilized was a protein with UniProt ID P04626, belonging to the ErbB2 receptor tyrosine kinase group, with FMM as a reference ligand. Among the numerous models obtained, the model selected had the same reference ligand. The 5th model was chosen due to the highest Global Model Quality Estimate score of 0.74, among all models with the FMM ligand. The selected model corresponded to the receptor tyrosine-protein kinase ErbB4.

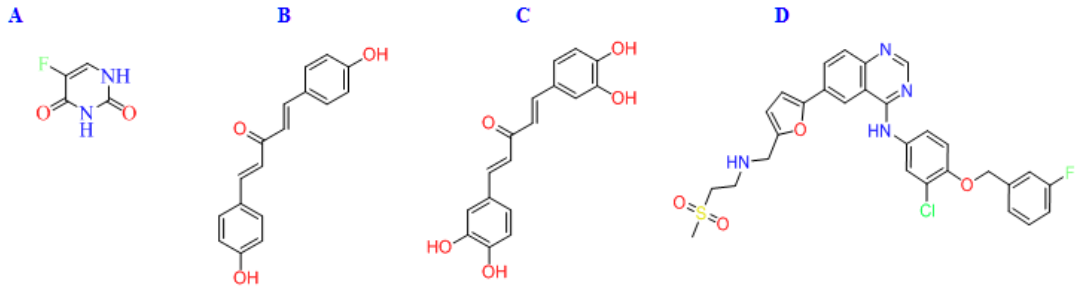

Fig. 1. The chemical structures of (A) 5-FU; (B) AC01; (C) AC02; (D) FMM. 5-FU, 5-Fluorouracil; AC01, (1E,4E)-1,5-bis (4-hydroxyphenyl) penta-1,4-dien-3-one; AC02, (1E,4E)-1,5-bis (3,4-dihydroxyphenyl) penta-1,4-dien-3-one; FMM, lapatinib.

Docking preparation and validation

Ligand preparation was carried out using Open Babel and AutoDockTools (15). The preparation of the protein target, including the addition of hydrogen atoms and partial charges, was performed using Discovery Studio 2022 Client version. Identification of the binding site or active site on the ErbB4 protein where the native ligand binds was also accomplished using Discovery Studio Visualizer software.

Redocking of the reference ligand, single docking of AC01, AC02, and 5-FU, and simultaneous docking of the combination of the 3 ligands with FMM were performed under similar parameters, using a grid box of sizes 40, 40, and 40 Å, with the center of the reference ligand as the center point of the grid box.

Redocking of the reference ligand was performed to validate the binding site of ErbB4. FMM was used as the reference ligand for the ErbB4 protein model used in this study. Redocking aimed to verify whether a ligand could be redocked into the active site of a target molecule with the appropriate position and orientation (16). Through redocking, we could assess how well the docking simulation replicated the correct position and orientation of a known ligand within the co-crystallized complex with the target molecule. One of the techniques used for validation was the comparison of binding poses, where the predicted binding poses of the redocked ligand were compared to the experimentally determined binding pose in the crystal structure. The alignment and similarity between the redocked pose and the crystallographic pose were then evaluated.

Single ligand docking

Automated docking was employed to study the binding of various drug molecules to the active site of ErbB4. AutoDock Vina version 1.2.3 utilized a semi-empirical free energy force field as an evaluation function to assess docked conformation solutions. Evaluation functions included pairwise evaluation and entropy changes during binding. The genetic algorithm method implemented in AutoDock Vina (17), was used to explore suitable binding modes of ligands in different conformations. Individual docking was performed for the natural ligand of the protein of B-cell lymphoma 2, ligands AC01, AC02, 5-FU, and FMM. The binding affinity and binding pose analysis to elucidate interactions between the protein and ligands, including hydrogen bonds, hydrophobic interactions, and π-π stacking were conducted using Discovery Studio Visualizer 2022.

Docking with multiple ligand simultaneous docking

We conducted simultaneous binding studies to compare the binding orientations of individual ligands and ligand pairs. Docking with multiple ligand simultaneous docking (MLSD) was also performed using AutoDock Vina. MLSD was used for the ligands FMM-AC01, FMM-AC02, and FMM-5-FU pairs. The MLSD output was then analyzed for affinity and binding pose.

Multiple ligand simultaneous molecular dynamics

Molecular dynamics (MD) simulations are a critical tool in computational chemistry that allows us to model the movement of atoms within molecules and understand how they interact over time. This study utilized MD simulation methods to understand the interaction between compounds AC01 and

AC02 with the ErbB4 protein. MD simulations were also conducted using the simultaneous approach, where a complex of dual ligands with ErbB4 was simulated to study stability over 100 ns. The binding free energy during MD simulations was calculated using the Molecular Mechanics/Poisson-Boltzmann Surface Area (MM-PBSA) approach. MD simulations were performed using the GROMACS 2023.2 software package (18,19), and energy decomposition was conducted by means of the gmx_MMPBSA version 1.6.2 (20).

The best model based on the docking results of ligands with the ErbB4 protein was chosen as the starting point for MD simulations. The AMBER99SB-ILDN force field (21) was selected to create the protein topology, and the topology of the ligands was generated using the Amber force field with the assistance of the ACPYPE version 2022.7.21 package (22). Placement of the protein-ligand complex system in a water box employed the transferable intermolecular potential with 3 points water model, with a minimum distance of approximately 10 Å between the protein and the box edges. System neutralization was achieved by adding Cl^- ions to the system box using the Monte-Carlo ion placement method. System equilibration was conducted in 2 stages namely the NVT ensemble (defined as the number of particles, volume, and temperature), followed by the NPT ensemble (defined as the number of particles, pressure, and temperature). The production phase lasted for 100 ns.

The results of multiple ligand simultaneous MD simulations were then examined through various parameters, including root mean square deviation (RMSD), root mean square fluctuation (RMSF), radius of gyration (RG), solvent accessible surface area (SASA), free energy binding, and energy decomposition (23). RMSD is the measurement of the deviation between the positions of atoms in a protein or ligand structure at different time points during the simulation. It was used to assess the system stability and to compare the structures obtained from various simulations. RMSF is a measure of the deviation of the position of each atom in a protein or ligand structure from its average position during the simulation. It was used to assess the flexibility of system and to identify regions that were more flexible or rigid.

The RG is a measure of the compactness of a protein or ligand structure. It was calculated as the root mean square distance of each atom in the structure from the center of mass. SASA is a measure of the surface area of a protein or ligand structure that is accessible to solvent molecules. It was used to assess the exposure of different regions of the structure to the solvent. Free energy binding is a measure of the strength of the interaction between a ligand and a protein. It was calculated using methods such as MM-PBSA (24). Additionally, energy decomposition was calculated by gmx-MM-PBSA (20) which is a method to calculate the energy contribution of individual residues or groups of residues in a molecular system. Per-residue decomposition analysis is a type of energy decomposition that calculates the energy contribution of single residues by summing its interactions over all residues in the system.

RESULTS

Dual ligand molecular docking

Redocking is a common procedure used to validate docking results by removing the ligand from the complex, repeating the docking process, and comparing the generated pose with the crystal structure. There are several approaches to assess the success of redocking, such as defining the ratio of samples where the RMSD of the top-ranked pose is less than 2 Å. The smaller the average RMSD value of the top-ranked poses, the better the performance of the scoring function or model. Another approach is the comparison of binding poses, where the predicted binding pose of the redocked ligand is compared to the experimentally determined binding pose in the crystal structure. The alignment and similarity between the redocked pose and the crystallographic pose are then evaluated.

Visualization of the results of redocking the reference ligand (FMM) to the active site of ErbB4 is shown in Fig. 2A. Based on RMSD calculations, the change in the position of the reference ligand between the redocked pose and the crystallographic pose was within 1.351 Å. This indicated that the docking procedure used was valid, and the docking parameters could be used as a reference for docking test ligands, and the results obtained could be trusted.

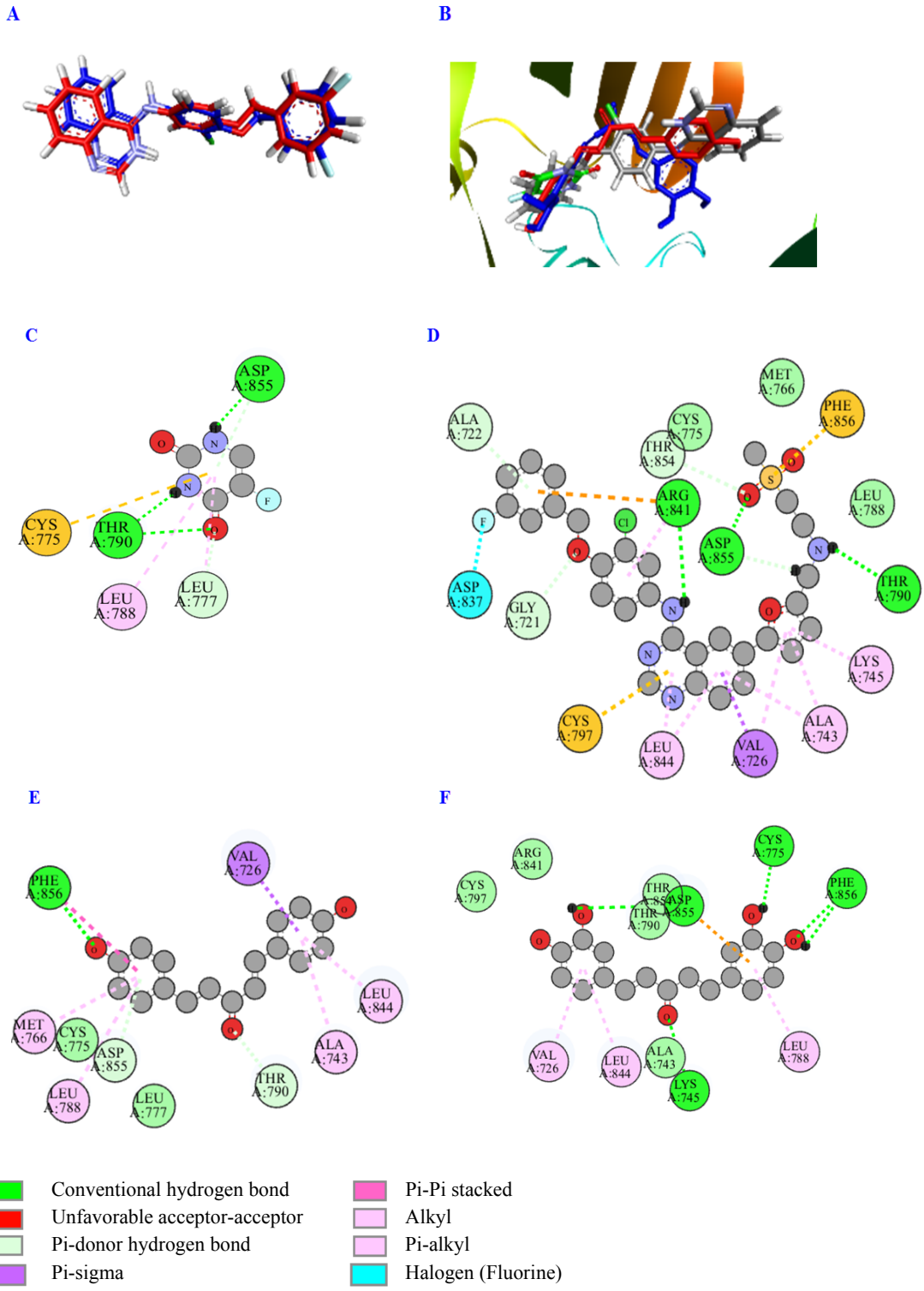

Fig. 2. (A) Overlay of the FMM structure in the redocked pose (red carbon) and the crystallographic pose (blue carbon); (B) overlay of FMM, 5-FU, AC01, and AC02 within the ErbB4 cavity; visualization of the residual interactions of ErbB4 with (C) 5-FU; (D) FMM; (E) AC01; and (F) AC02. 5-FU, 5-Fluorouracil; AC01, (1E,4E)-1,5-bis (4-hydroxyphenyl) penta-1,4-dien-3-one; AC02, (1E,4E)-1,5-bis (3,4-dihydroxyphenyl) penta-1,4-dien-3-one; FMM, lapatinib.

Table 1 summarized the molecular docking results for both single ligands and multi-ligands. A lower binding affinity value indicated a stronger interaction between the ligand and its target. Three-dimensional visualization (Fig. 2B) showed that individual docking results for AC01, AC02, and 5-FU could occupy the binding cavity of ErbB4, similar to the position of FMM. AC01 and AC02 could occupy the active site of ErbB4 in a manner resembling the position of FMM, while 5-FU, due to its molecular size, only occupied a part of FMM, specifically in the quinoline ring binding to the fluorine element. 5-FU was able to form 3 hydrogen bonds with active site residues of ErbB4, namely 2 bonds with Thr790 and 1 with Asp855 (Fig. 2C). A similar pattern was observed with FMM (Fig. 2D), which could interact with both of these residues, albeit in different forms of interactions, van der Waals interaction with Thr-790, while ASP855 formed an interaction with the fluorine halogen. Overall, both ligands targeting the same active site exhibited various interactions, but the molecular size of 5-FU resulted in lower affinity (-5.188 Kcal/mol) compared to FMM (-9.926 Kcal/mol). 5-FU did not reach the larger portion of the other active site of ErbB2, making it unable to induce enzymatic activity from ErbB4. In contrast, AC01 and AC02 showed different behaviour. Both ligands occupied the active site of ErbB4 similar to FMM. The clear overlap observed among all 4 ligands in Fig. 2B highlighted their structural similarity and suggested consistent binding conformations within the active site. Moreover, the residual description of ErbB4 in interaction with AC01 and AC02 was shown in Fig. 2E and Fig. 2F, respectively.

Table 1 summarizes the binding affinities of simultaneous docking of ErbB4 with 3 ligand pairs. The FMM-5-FU pair exhibited the strongest affinity at -13.893 Kcal/mol. The FMM-AC01 and FMM-AC02 pairs were slightly weaker at -12.880 and -12.637 Kcal/mol, respectively.

Interesting phenomena were shown in simultaneous docking (Fig. 3A-3G). The presence of 2 ligands simultaneously on ErbB4 disrupted the binding orientation of one of the ligands to the active site. The FMM-5-FU pair showed that FMM could occupy the ErbB4 activation loop, while 5-FU was located far from the active site (Fig. 3A and 3B). The AC01-FMM and AC02-FMM pairs demonstrated that AC01 and AC02 occupied the activation loop, while FMM in both pairs was located outside the activation loop (Fig. 3C-3G). This indicated the ability of AC01 and AC02 to synergize with FMM, allowing them to act as agonists or antagonists of FMM targeting ErbB4, which of course, requires experimental validation.

Table 1. Single and dual ligand molecular docking binding affinity.

Ligand	Binding affinity (Kcal/mol)	Single or dual ligand molecular docking
5-FU	-5.188	Single
AC01	-8.521	Single
AC02	-8.392	Single
FMM-5-FU	-13.893	Dual
FMM-AC01	-12.880	Dual
FMM-AC02	-12.637	Dual
FMM	-9.926	Single

5-FU, 5-Fluorouracil; AC01, (1E,4E)-1,5-bis (4-hydroxyphenyl) penta-1,4-dien-3-one; AC02, (1E,4E)-1,5-bis (3,4-dihydroxyphenyl) penta-1,4-dien-3-one; FMM, lapatinib.

A

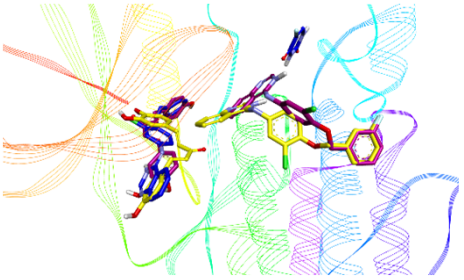

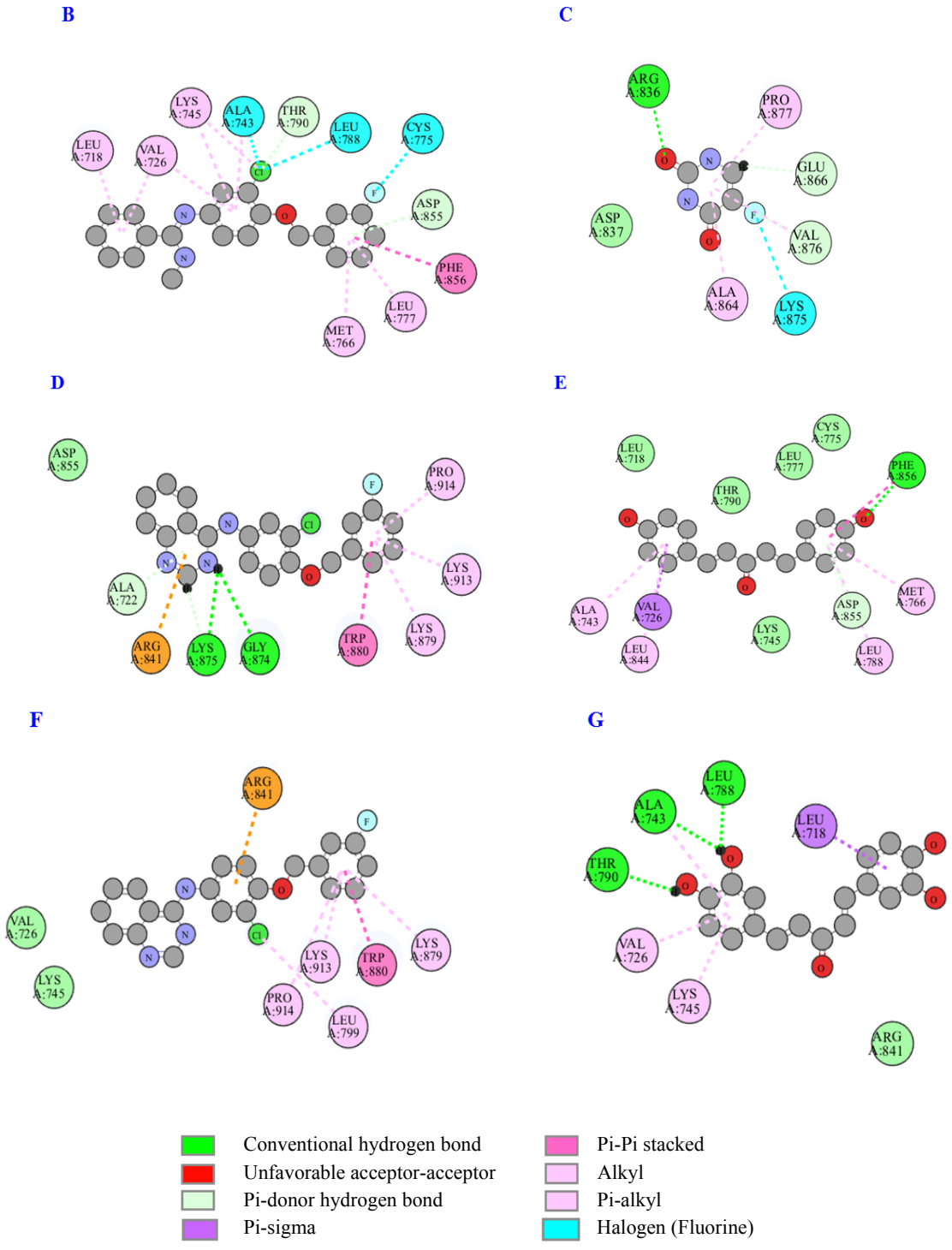

Fig. 3. (A) Overlap dual ligand simultaneous docking of FMM-5-FU (blue carbon) pair, FMM-AC01 (red), and FMM-AC02 (yellow); (B) and (C) ErbB4 residue interactions with the FMM-5-FU pair; (D) and (E) with the FMM-AC01 pair; (F) and (G) with the FMM-AC02 pair. 5-FU, 5-Fluorouracil; AC01, (1E,4E)-1,5-bis (4-hydroxyphenyl) penta-1,4-dien-3-one; AC02, (1E,4E)-1,5-bis (3,4-dihydroxyphenyl) penta-1,4-dien-3-one; FMM, lapatinib.

Dual ligand simultaneous MD

RMSD analysis

The movement of ErbB4 protein molecules and ligands during the simulation was illustrated in Fig. 4A-4C. The 3 complexes (protein-FMM-AC01, protein-FMM-AC02, and protein-FMM-5-FU) during the 100 ns simulation exhibited low RMSD values. This indicated that the interaction between ErbB4 and the ligand pairs FMM-AC01, FMM-AC02, and FMM-5-FU formed stable complexes. The presence of both ligands did not impact the stability of ligand binding on the active site of ErbB4. RMSD values less than 0.5 Å suggested that each complex tended to maintain its binding conformation throughout the simulation.

RMSF analysis

Fluctuations of atomic and amino acid residues comprising the ErbB4 protein in its interaction with the ligand pairs FMM-AC01, FMM-AC02, and FMM-5-FU were observed through RMSF measurements of the protein. The summarized results of the RMSF measurements in Fig. 4D indicated the fluctuations in protein residues within the range of amino acids 850 to 975. These residues corresponded to the ErbB4 activation loop. Other residues were displayed in the outer area of the activation loop, specifically amino acid sequences 725 to 775, but with lower movement values. This suggested that the 3 ligand pairs tended to form interactions with the activation loop of ErbB4. In other words, residues 850 to 975 and 725 to 775 depicted the parts of ErbB4 that exhibited flexibility due to their interactions with the ligands.

SASA analysis

There was no change in the surface area of the ErbB4 biomolecule during its interaction with ligand pairs. The results of SASA calculations for ErbB4 in complex with the ligand pairs FMM-AC01, FMM-AC02, and FMM-5-FU during a 100 ns MD simulation showed no substantial alteration in the surface area of protein. The surface area remained constant from the beginning to the end of the simulation. Figure 4E, summarizing the measurement of the surface area of protein during the simulation, indicated that the protein-ligand binding was relatively stable, and there was no change in the molecular conformation of the protein. This suggested the stability of the molecular structure of ErbB4 and the robustness of the protein-ligand interactions.

RG analysis

Similar to the SASA parameter, the RG values for the system in the ErbB4 complex with 3 ligand pairs (FMM-AC01, FMM-AC02, and FMM-5-FU), as depicted in Fig. 4F, showed minor changes compared to the initial state during simulations. This condition provided insight that the shape and dynamics of the molecules constituting the system underwent minimal movements that could induce conformational changes, alterations in binding modes with ligands, or structural damage to the protein or ligand pairs.

Binding free energy

The free energy binding calculations for the ErbB4 complex with 3 ligand pairs were conducted using the MM-PBSA approach. The average of Gibbs free energy (ΔG) calculations for the ErbB4 complex with the FMM-AC01, FMM-AC02, and FMM-5-FU pairs was depicted in Fig. 4G. FMM-5-FU (-48.38 Kcal/mol) exhibited a more negative binding free energy, indicating a stronger binding affinity compared to FMM-AC01 and FMM-AC02. The ErbB4 complex with the FMM-AC02 pair (-44.36 Kcal/mol) demonstrated a stronger binding than FMM-AC01 (-31.91 Kcal/mol).

Energy decomposition

The binding free energy formed in a protein-ligand complex was the contribution of interactions of each residue in the protein that was within a sufficient range to form interactions. Energy decomposition analysis during MD simulations of the ErbB4 complex with the ligand pairs FMM-AC01, FMM-AC02, and FMM-5-FU was performed for residues within up to 6 Å.

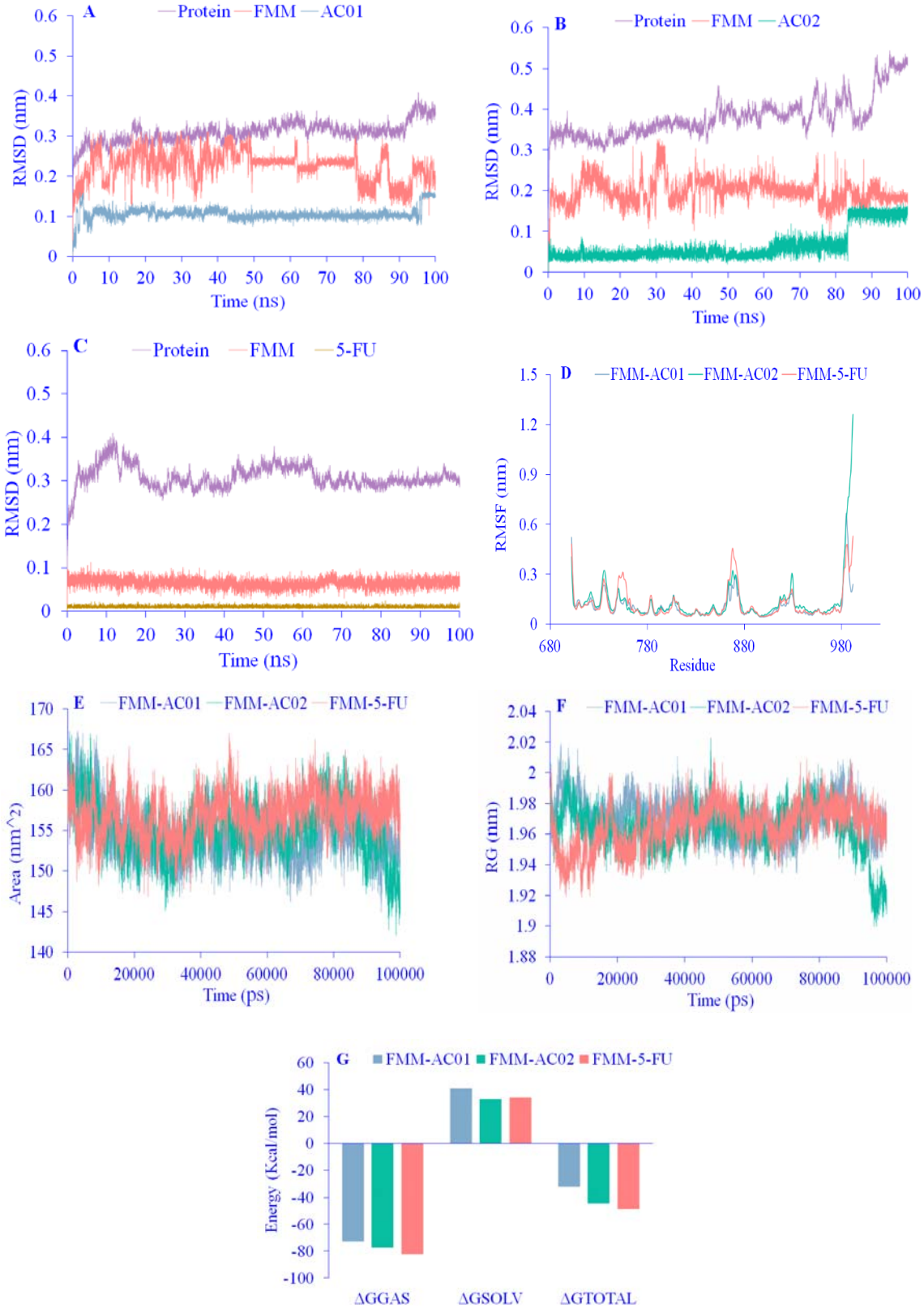
A
Protein
FMM
AC01
RMSD (nm)
Time (ns)
B
Protein
FMM
AC02
RMSD (nm)
Time (ns)
C
Protein
FMM
5-FU
RMSD (nm)
Time (ns)
D
FMM-AC01
FMM-AC02
FMM-5-FU
RMSF (nm)
Residue
E
FMM-AC01
FMM-AC02
FMM-5-FU
Area (nm^2)
Time (ps)
F
FMM-AC01
FMM-AC02
FMM-5-FU
RG (nm)
Time (ps)
G
FMM-AC01
FMM-AC02
FMM-5-FU
Energy (Kcal/mol)
ΔGGAS
ΔGSOLV
ΔGTOTAL

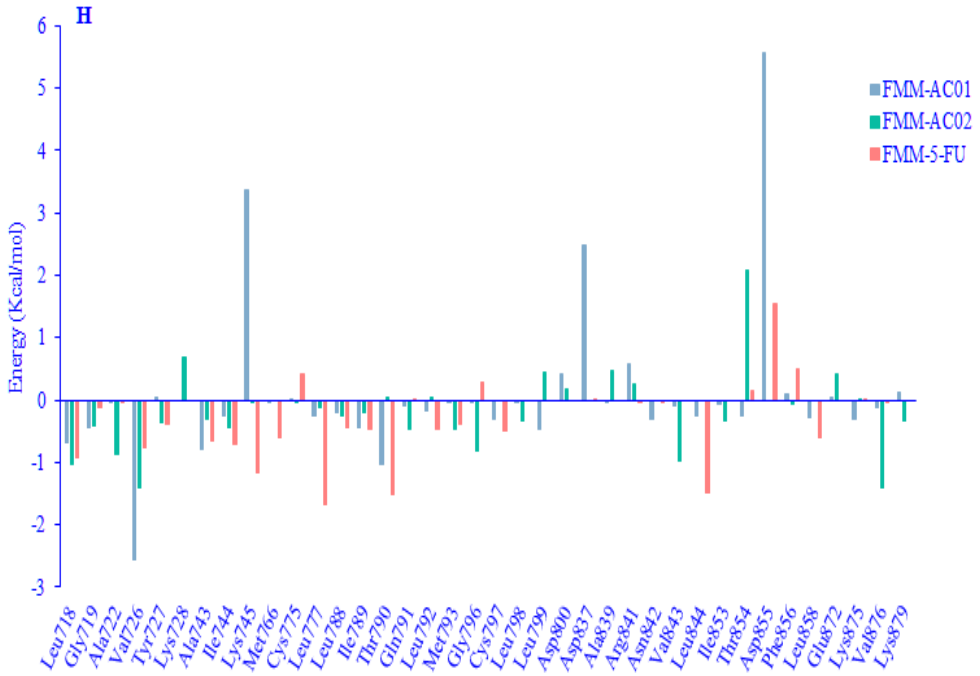

Fig. 4. Molecular dynamics simulation. (A-C) RMSD in AC01, AC02, and 5-FU, respectively; (D) RMSF; (E) SASA; (F) RG; (G) binding free energy; (H) residual decomposition energy. 5-FU, 5-Fluorouracil; AC01, (1E,4E)-1,5-bis (4-hydroxyphenyl) penta-1,4-dien-3-one; AC02, (1E,4E)-1,5-bis (3,4-dihydroxyphenyl) penta-1,4-dien-3-one; FMM, lapatinib; RMSD, root mean square deviation; RMSF, root mean square fluctuation; RG, radius of gyration; SASA, solvent accessible surface area; ΔG, Gibbs free energy.

The results are summarized in Fig. 4H. It could be observed that the FMM-AC01 ligand pair had strong interactions with Val726 (-2.567 Kcal/mol) and Thr790 (-1.037 Kcal/mol). Both amino acids were residues outside the activation loop of ErbB2. In contrast, interactions with active site residues of ErbB2 such as Leu858, Leu844, and Thr854 only provided binding energies below 0.3 Kcal/mol. On the other hand, the activation loop residues of ErbB4, Asp837 (+2.479 Kcal/mol), and Asp855 (+5.563 Kcal/mol) showed repulsive interactions. Furthermore, non-active site interactions, such as Lys745 (+3.365 Kcal/mol), also contributed to the positive energy of the complex.

DISCUSSION

In a single-ligand docking experiment, it was observed that 5-FU exhibited the lowest binding affinity, while FMM showed the highest binding affinity. The visual inspection of the docking results indicated that AC01, AC02, and 5-FU could occupy the ErbB4 activation loop, similar to FMM. In simultaneous dual-ligand docking, the FMM-5-FU pair displayed the strongest affinity. This combination maintained FMM within the activation loop while positioning 5-FU outside the loop. The FMM-AC01 and FMM-AC02 pairs exhibited slightly weaker binding affinities compared to FMM-5-FU. However, both AC01 and AC02 could occupy the ErbB4 activation loop, while FMM in combination with both ligands remained outside the loop.

Most activation loops in ErbB4 bound by FMM encompass residues 844 to 857 (25). Consequently, AC01 and AC02 displayed potential interactions with the ErbB4 activation loop, as illustrated in Fig. 2E and 2F. Both curcumin analogs were capable of forming hydrogen bonds with Phe856. However, AC02 formed conventional hydrogen bonds with Asp855, and AC01 only created hydrogen bond donor interactions with this residue. Overall, AC01 and AC02 exhibited similar interactions with the activation loop residues of ErbB4.

Furthermore, the FMM-AC02 pair showed dominance in non-activation loop residues, contributing to binding energy. Only one activation loop residue, Leu844, contributed -0.984 Kcal/mol (with the highest being -1.416 Kcal/mol). Several activation loop residues also formed interactions with the ligands but in smaller quantities and magnitudes than non-activation loop residues. Similar to the FMM-AC01 pair, the activation loop residue Asp855 also exhibited positive interaction energy, which was 2.086 Kcal/mol.

Although single-ligand docking indicated that FMM had a stronger binding affinity than AC01 or AC02, MD results confirmed that the average free binding energy of AC01 was higher than that of FMM. Furthermore, AC01 and AC02 combined with FMM showed promising stability based on MD results. This study provided the best opportunities for AC01 and AC02 to be further investigated as potential anticancer candidates through ErbB4 inhibition.

CONCLUSION

The docking experiments revealed that 5-FU had the lowest binding affinity, while FMM exhibited the highest binding affinity for ErbB4. Visually, the docking results demonstrated that AC01, AC02, and 5-FU could effectively occupy the ErbB4 activation loop. AC02 showed marginally more robust interactions with the ErbB4 activation loop than AC01. MD simulations employing the MM-PBSA approach revealed that AC01 exhibited a higher average binding free energy than AC02. Furthermore, in simulations, AC01 and AC02 exhibited encouraging stability when combined with FMM. The observations indicate that AC01 and AC02 have the potential to act as anticancer candidates, demonstrating both only and synergetic inhibition of ErbB4 when combined with FMM.

Acknowledgments

This research was funded by the Ministry of Education, Culture, Research, and Technology of Indonesia through Penelitian Fundamental-Reguler (PRF) 2024 *via* Decree of Rector of Universitas Negeri Gorontalo No. 063/E5/PG.02.00.PL/2024 under contract No. 925/UN47.D1.1/PT.01.03/2024.

Conflicts of interest statement

All the authors declared no conflicts of interest.

Authors' contributions

All the authors had equally contributed to the current study. All authors read and approved the finalized version.

REFERENCES

1. Cancer research UK worldwide cancer statistics. Available: https://www.cancerresearchuk.org/health-professional/cancer-statistics/worldwide-cancer (accessed on 8 September 2023).
2. World health organization cancer. Available: https://www.who.int/news-room/fact-sheets/detail/cancer (accessed on 8 September 2023).
3. World cancer research fund international worldwide cancer data. Available: https://www.wcrf.org/cancer-trends/worldwide-cancer-data (accessed on 8 September 2023).
4. Sung H, Ferlay J, Siegel RL, Laversanne M, Soerjomataram I, Jemal A, *et al*. Cancer statistics 2020: GLOBOCAN estimates of incidence and mortality worldwide for 36 cancers in 185 countries. CA Cancer J Clin. 2021;71(3):209-249. DOI: 10.3322/caac.21660.
5. Sundvall M, Iljin K, Kilpinen S, Sara H, Kallioniemi OP, Elenius K. Role of ErbB4 in breast cancer. J Mammary Gland Biol Neoplasia. 2008;13(2): 259-268. DOI: 10.1007/s10911-008-9079-3.
6. Canfield K, Li J, Wilkins OM, Morrison MM, Ung M, Wells W, *et al*. Receptor tyrosine kinase ERBB4 mediates acquired resistance to ERBB2 inhibitors in breast cancer cells. Cell Cycle. 2015;14(4):648-655. DOI: 10.4161/15384101.2014.994966.
7. Bose R, Zhang X. The ErbB kinase domain: structural perspectives into kinase activation and inhibition. Exp Cell Res. 2009;315(4):649-658. DOI: 10.1016/j.yexcr.2008.07.031.
8. Gerbin CS. Activation of ERBB receptors. Available: https://www.nature.com/scitable/topicpage/activation-of-erbb-receptors-14457210/ (accessed on 8 September 2023).
9. Collins DM, Conlon NT, Kannan S, Verma CS, Eli LD, Lalani AS, *et al*. Preclinical characteristics of the irreversible Pan-HER kinase inhibitor neratinib compared with lapatinib: implications for the treatment of HER2-positive and HER2-mutated breast cancer. Cancers (Basel). 2019;11(6):737,1-27. DOI: 10.3390/cancers11060737.
10. Black LE, Longo JF, Carroll SL. Mechanisms of receptor tyrosine-protein kinase ErbB-3 (ERBB3) action in human neoplasia. Am J Pathol. 2019;189(10):1898-1912. DOI: 10.1016/j.ajpath.2019.06.008.

11. Li H, Li C. Multiple ligand simultaneous docking: orchestrated dancing of ligands in binding sites of protein. J Comput Chem. 2010;31(10):2014-2022. DOI: 10.1002/jcc.21486.
12. Gupta A, Chauhan SS, Gaur AS, Parthasarathi R. Computational screening for investigating the synergistic regulatory potential of drugs and phytochemicals in combination with 2-deoxy-d-glucose against SARS-CoV-2. Struct Chem. 2022;33(6):2179-2193. DOI: 10.1007/s11224-022-02049-0.
13. O'Boyle NM, Banck M, James CA, Morley C, Vandermeersch T, Hutchison GR. Open babel: an open chemical toolbox. J Cheminform. 2011;3:33,1-14. DOI: 10.1186/1758-2946-3-33.
14. Waterhouse A, Bertoni M, Bienert S, Studer G, Tauriello G, Gumienny R, *et al*. Swiss-model: homology modelling of protein structures and complexes. Nucleic Acids Res. 2018;46:W296-W303. DOI: 10.1093/nar/gky427.
15. Morris GM, Huey R, Lindstrom W, Sanner MF, Belew RK, Goodsell DS, *et al*. Autodock4 and autodocktools4: automated docking with selective receptor flexibility. J Comput Chem. 2009;30(16):2785-2791. DOI: 10.1002/jcc.21256.
16. Ischak NI, Aman LO, Hasan H, Kilo Ala, Asnawi A. In Silico screening of *Andrographis paniculata* secondary metabolites as anti-diabetes mellitus through PDE9 inhibition. Res Pharm Sci. 2023;18(1):100-111. DOI: 10.4103/1735-5362.363616.
17. Eberhardt J, Santos-Martins D, Tillack AF, Forli S. Autodock vina 1.2.0: new docking methods, expanded force field, and python bindings. J Chem Inf Model. 2021;61(8):3891-3898. DOI: 10.1021/acs.jcim.1c00203.
18. Van Der Spoel D, Lindahl E, Hess B, Groenhof G, Mark AE, Berendsen HJC. GROMACS: fast, flexible, and free. J Comput Chem. 2005;26(16):1701-1718. DOI: 10.1002/jcc.20291.
19. Pronk S, Páll S, Schulz R, Larsson P, Bjelkmar P, Apostolov R, *et al*. GROMACS 4.5: a high-throughput and highly parallel open source molecular simulation toolkit. Bioinformatics 2013;29(7):845-854. DOI: 10.1093/bioinformatics/btt055.
20. Valdés-Tresanco MS, Valdés-Tresanco ME, Valiente PA, Moreno E. Gmx_MMPBSA: a new tool to perform end-state free energy calculations with GROMACS. J Chem Theory Comput. 2021;17(10):6281-6291. DOI: 10.1021/acs.jctc.1c00645.
21. Lindorff-Larsen K, Piana S, Palmo K, Maragakis P, Klepeis JL, Dror RO, *et al*. Improved side-chain torsion potentials for the Amber ff99SB protein force field. Proteins. 2010;78(8): 1950-1958. DOI: 10.1002/prot.22711.
22. Da Silva AWS, Vranken WF. ACPYPE-antechamber python parser interface. BMC Res Notes. 2012;5(367):1-8. DOI: 10.1186/1756-0500-5-367.
23. Durrant JD, McCammon JA. Molecular dynamics simulations and drug discovery. BMC Biol. 2011;9(71):1-9. DOI: 10.1186/1741-7007-9-71.
24. Miller BR 3rd, McGee TD Jr, Swails JM, Homeyer N, Gohlke H, Roitberg AE. MMPBSA.Py: an efficient program for end-state free energy calculations. J Chem Theory Comput. 2012;8(9):3314-3321. DOI: 10.1021/ct300418h.
25. Qiu C, Tarrant MK, Choi SH, Sathyamurthy A, Bose R, Banjade S, *et al*. Mechanism of activation and inhibition of the HER4/ErbB4 kinase. Structure. 2008;16(3):460-467. DOI: 10.1016/j.str.2007.12.016.